To appear in *Liquid Crystals*
Vol. 00, No. 00, Month 20XX, 1–8

Supporting Material

An Investigation into the Hexagonal Phases Formed in High-Concentration Dispersions of Well-Defined Cylindrical Block Copolymer Micelles

D.W. Hayward[a,b,c], G.R. Whittell[b], J.B. Gilroy[b,d], I. Manners[b] and R.M. Richardson[a*]

[a]*H.H. Wills Physics Laboratory, University of Bristol, Bristol BS8 1TL, U.K.*; [b]*School of Chemistry, University of Bristol, Cantock's Close, Bristol BS8 1TS, U.K.*; [c]*Bristol Centre for Functional Nanomaterials, University of Bristol, Bristol BS8 1TL, U.K.*; [d]*Department of Chemistry, The University Western Ontario, London, Ontario Canada, N6A 5B7*

(*Received 00 Month 20XX; final version received 00 Month 20XX*)

1. Hexagonal Structure Factor Model

The following is a brief overview of paracrystals in general and the outline for deriving the paracrystalline structure factor for a 2-dimensional hexagonal lattice. A more complete derivation is provided in [1] and [2].

1.1 *Hosemann's Theory of Paracrystals in One Dimension*

A paracrystalline structure is one that is subject to lattice distortions of the second kind, that is although it possesses short range order, the nearest neighbour distances are not identical. Instead, these distances follow a distribution function governed by the shape of the structural units and the interaction between them. This is in contrast to distortions of the first kind, where the equilibrium positions of all neighbours, near and distant, are fixed at the nodes of the crystalline lattice. If the distribution function of nearest neighbours, $H_1(x)$, is known, it is possible to calculate the mean distance between nearest neighbours:

$$a = \int x H_1(x)\,\mathrm{d}x \tag{S1}$$

as well as the position of the next nearest neighbour by convoluting $H_1(x)$ with itself, displaced by a distance x':

$$H_2(x) = \int_0^\infty H_1(x')H_1(x-x')\,\mathrm{d}x' = H_1 \otimes H_1 \tag{S2}$$

Repeating this convolution step gives rise to the positions of the third nearest neighbours:

$$H_3(x) = H_2 \otimes H_1 = H_1 \otimes H_1 \otimes H_1 = H_1 \overset{3}{\otimes} H_1 \tag{S3}$$

*Corresponding author. Email: robert.richardson@bristol.ac.uk

whereby it may be seen that the positions of the n-th nearest neighbours may be found via n self-convolutions of $H_1(x)$ and the total distribution function is the sum of these convolutions:

$$S(x) = H_0 + \sum_{n=1}^{\infty} H_1 \overset{n}{\otimes} H_1 + H_{-1} \overset{n}{\otimes} H_{-1} \tag{S4}$$

where H_0 is a delta function at the origin and H_{-1} is the distribution of nearest neighbours in the negative direction, required for centrosymmetry.

The expected diffraction pattern of the paracrystalline lattice described above is simply the Fourier transform of S. It can be expressed in terms of the transform of H_1 as::

$$\mathcal{F}[H_1(x)] = F(Q_x) \tag{S5}$$

where $Q(x)$ is the scattering vector in the x direction. The convolution theorem states that the Fourier transform of a convolution is the product of transforms of the convoluted functions i.e.

$$\mathcal{F}[H_2(x)] = F^2(Q_x) \tag{S6}$$

To a first approximation, the distribution H_1 can be represented by a Gaussian curve with width Δ, such that:

$$H_1(x+a) = \frac{1}{\sqrt{2\pi}\Delta} e^{-\frac{1}{2}(x^2/\Delta^2)} \tag{S7}$$

The Fourier transform of which is also a Gaussian:

$$F = e^{-2\pi^2 Q_x^2 \Delta^2} \tag{S8}$$

Applying the convolution theorem to (S4) and summing the series, one arrives at the following functional form:

$$S(Q_x) = \mathrm{Re}\left(\frac{1+F(Q_x)}{1-F(Q_x)}\right) \tag{S9}$$

which, when combined with the Gaussian approximation in (S7) and (S8) is shown graphically in Figure S1. It can be seen that the amplitude of the peaks decays and the peak width increases with increasing Q, however the position of the peaks remains at $2n\pi/a$.

1.2 *Extension to Multiple Dimensions*

The same principles can easily be extended to cover an orthogonal, two- or three-dimensional coordinate system. In this case, the Gaussian approximation of the original pair distribution for first neighbours, as described in (S7), becomes:

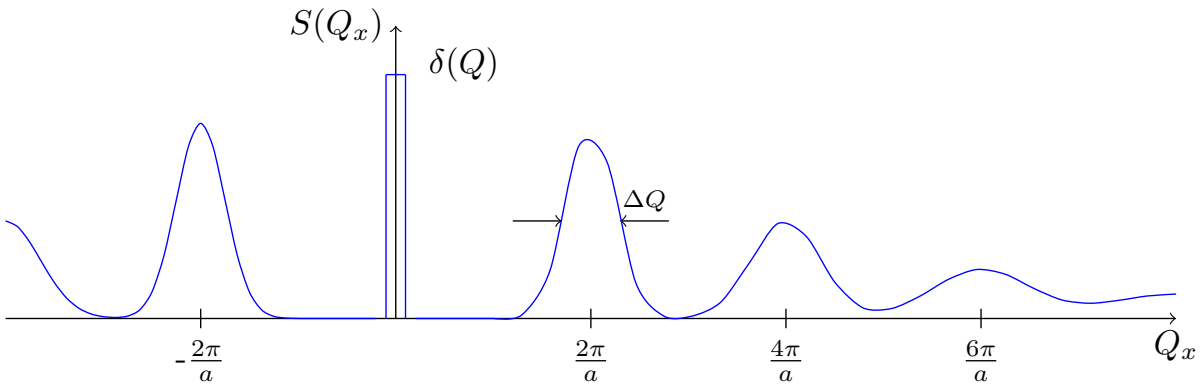

Figure S1. Schematic of the 1-dimensional structure factor $S(Q_x)$ as a function of the scattering vector Q_x.

$$H_1(\mathbf{r}+\mathbf{a}) = \frac{1}{(2\pi)^{\frac{3}{2}}\Delta_{1x}\Delta_{1y}\Delta_{1z}} \exp\left[-\frac{1}{2}\left(\frac{x^2}{\Delta_{1x}^2}+\frac{y^2}{\Delta_{1y}^2}+\frac{z^2}{\Delta_{1z}^2}\right)\right] \tag{S10}$$

where the subscripts 1x, 1y and 1z refer to displacements from axis 1 in the x, y and z direction respectively. The Fourier transform of (S10) is:

$$\mathcal{F}[H_1(\mathbf{r}+\mathbf{a})] = F_1(\mathbf{Q}) = \exp[-2\pi^2(\Delta_{1x}^2Q_x^2+\Delta_{1y}^2Q_y^2+\Delta_{1z}^2Q_z^2)] \tag{S11}$$

where $\mathbf{Q}$ is the scattering vector in the reciprocal lattice. By analogy with (S9), the overall expected diffraction pattern is then given by:

$$S(\mathbf{Q}) = \prod_{k=1,2,3} \mathrm{Re}\left(\frac{1+F_k(\mathbf{Q})}{1-F_k(\mathbf{Q})}\right) \tag{S12}$$

Note that here the subscript (k) refers to each of the three orthogonal lattice vectors as opposed to the order of nearest neighbours as in the one dimensional case. This formula applies to the case of an ideal paracrystal where the unit cells of the prefect crystals are always distorted into parallelepipeds.

For the more general case of a real paracrystal, the distributions of the diagonals must be included. For a two dimensional net, with no correlation between the lattice vector 1 and the lattice vector 2 (i.e. a_1 and a_2), Hosemann has shown [1]:

$$S = 1 + 2\,\mathrm{Re}\left[\frac{F_{10}}{1-F_{10}}+\frac{F_{01}}{1-F_{01}}+\frac{F_{\bar{1}1}}{1-F_{\bar{1}1}}\cdot\frac{1-F_{\bar{1}0}F_{0\bar{1}}}{(1-F_{\bar{1}0})(1-F_{0\bar{1}})}+\frac{F_{\bar{1}0}}{1-F_{\bar{1}0}}\cdot\frac{F_{01}}{1-F_{01}}\right] \tag{S13}$$

where the subscripts represent the Miller indices of the reciprocal lattice.

1.3 *The Hexagonal Lattice*

In the main text, the case of a two-dimensional hexagonal lattice is discussed. A simple 2D hexagonal net may be defined using two lattice vectors $\mathbf{a_1}$ and $\mathbf{a_2}$ of identical magnitude, a, and separated

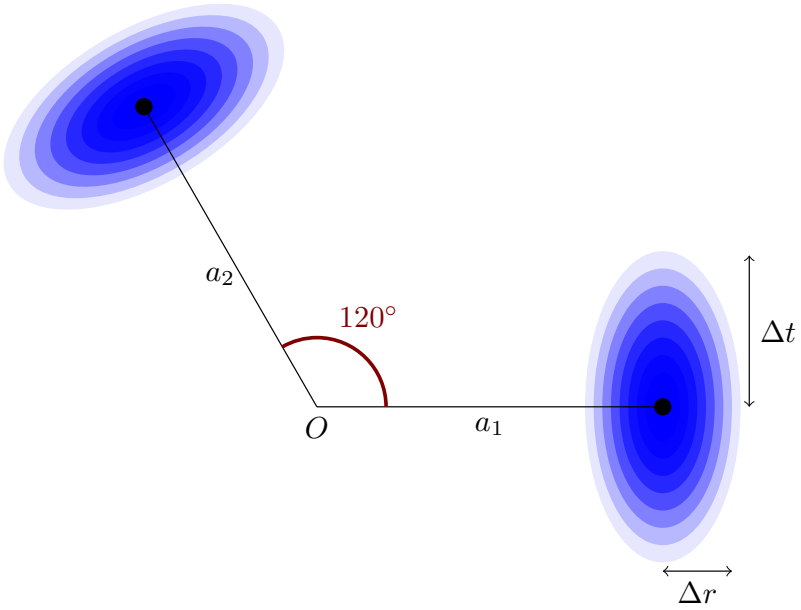

Figure S2. Diagram showing the lattice vectors and nearest neighbour distribution functions of a 2D hexagonal net.

by 120°. Following Hosemann, the reciprocal lattice of the 2D hexagonal net also takes the form of hexagonal lattice with lattice vectors $\mathbf{a_1^*}$ and $\mathbf{a_2^*}$ orthogonal to $\mathbf{a_1}$ and $\mathbf{a_2}$ respectively and of magnitude $4\pi/(\sqrt{3}a)$. The lattice distortions in a 2D hexagonal lattice may be represented by two pair distribution functions H_{10} and H_{01} as shown in Figure S2. Due to the symmetry of the system, this must also be averaged over all 6 possible orientations:

$$S_H = 1 + \sum_{k=1}^{6} \mathrm{Re}\frac{F_k}{(1-F_k)(1-F_{k-1})} \tag{S14}$$

When the six-fold symmetry is taken into account, the diagonal correlation H_{11} and H_{10} are determined by H_{01} and Hosemann has shown that the Fourier transforms for the first three axis directions of a 2D hexagonal net, assuming a Gaussian pair distribution function, can be calculated and are given by:

$$F_1(\mathbf{Q}) = e^{-iQ_x a_1} e^{-\frac{1}{2}(Q_x^2\Delta_r^2 + Q_y^2\Delta_t^2)} \tag{S15a}$$

$$F_2(\mathbf{Q}) = e^{-i(Q_x a_1 \cos\frac{\pi}{3} + Q_y a_1 \sin\frac{\pi}{3})} e^{-\frac{1}{2}(Q_x^2\Delta_r^2\cos^2\frac{\pi}{3} + Q_y^2\Delta_t^2\sin^2\frac{\pi}{3})} \tag{S15b}$$

$$F_3(\mathbf{Q}) = e^{-i(Q_x a_1 \cos\frac{2\pi}{3} + Q_y a_1 \sin\frac{2\pi}{3})} e^{-\frac{1}{2}(Q_x^2\Delta_r^2\cos^2\frac{2\pi}{3} + Q_y^2\Delta_t^2\sin^2\frac{2\pi}{3})} \tag{S15c}$$

where Q_x and Q_y are the components of $\mathbf{Q}$ in the 2D plane and Δr and Δt are the radial and transverse distortions respectively (as defined in Figure S2). F_{4-6} are the complex conjugates of F_{1-3} respectively (i.e. $F_4 = F_1^*$ and so on). It is worth noting here that, in contrast to rectangular lattices, the distribution function of node (1,1) is not the convolution of the (1,0) and (0,1) distribution functions, rather it is exactly identical to the (1,0) and (0,1) functions due to the hexagonal symmetry. In the method used by Hosemann and Bagchi, outlined above, the symmetry is restored by averaging over the 6 possible orientations, this is somewhat arbitrary and cannot be used to express the distribution functions in real space for example. A more elegant approach is provided

by Bousson and Doucet, [3] whereby the hexagonal symmetry is preserved throughout by defining the shape of the nearest neighbour distribution functions as the product of three Gaussians (of standard deviation σ). In the isotropic case (where $\Delta r = \Delta t = \Delta$), this ultimately leads to the equivalent result as attained by Hosemann, when $\Delta = \sqrt{2/3}\,\sigma$.

1.4 *Distribution of Lattice Parameters*

For flexible micelles, in addition to the distribution of lattice parameters arising from paracrystalline distortions in the lattice as given by (S1), it is postulated that there are regions within the lattice that are well crystallised and regions that are less well crystallised. This behaviour can be included very simply in (S16) by replacing the average lattice parameter a with some distribution of lattice parameters $g(a)$. It is also reasonable to assume that regions with larger lattice parameters will have greater distortions, hence the dependence of the distortion parameters on the lattice parameter, see equation (2) and Figure 4a in main text. To obtain the final structure factor for the whole paracrystal, the average over the distribution of lattice parameters is taken:

$$S(\mathbf{Q}) = \int g(a) S_H(\mathbf{Q}, a, \Delta r, \Delta t)\,\mathrm{d}a \tag{S16}$$

1.5 *Preferred Alignment*

For long rods in suspension, the total scattered intensity is given by:

$$I(Q) = \frac{2\pi L}{Q}(\rho \pi R)^2 \left\{ \frac{2J_1(QR)}{QR} \right\}^2 S(Q) \tag{S17}$$

where J_1 is the first order Bessel function, R, L and ρ are the radius, length and density of the rod and S(Q) is given by:

$$S(Q) = \frac{3}{\pi} \int_0^{\pi/3} f(\phi) S(Q_\perp, \phi)\,\mathrm{d}\phi \tag{S18}$$

where ϕ is the relative rotation around the long axis, as shown in Figure S3. If there is no preferred alignment, then $f(\phi) = 1$ and $S(Q)$ is independent of ϕ. If there is a preferred alignment in the system, this may be characterised by a trigonometric series in 6ϕ:

$$f(\phi) = 1 + c_6 \cos(6\phi) + c_{12} \cos(12\phi) + c_{18} \cos(18\phi) + ... \tag{S19}$$

In practice, it is only the c_6 term that meaningfully affects the $I(Q)$, the higher order terms may safely be neglected. When $c_6 > 0$, the amplitude of the first, third and fifth peaks (1, $\sqrt{4}$ and $\sqrt{9}$ respectively) are enhanced by the alignment and the second and sixth peaks ($\sqrt{3}$ and $\sqrt{12}$) are weakened. When $c_6 < 0$, this result is reversed. To achieve the fit shown in Figure 4 of the main text, a small preferred alignment correction was required. This alignment is probably imparted onto the sample by the walls of the capillary.

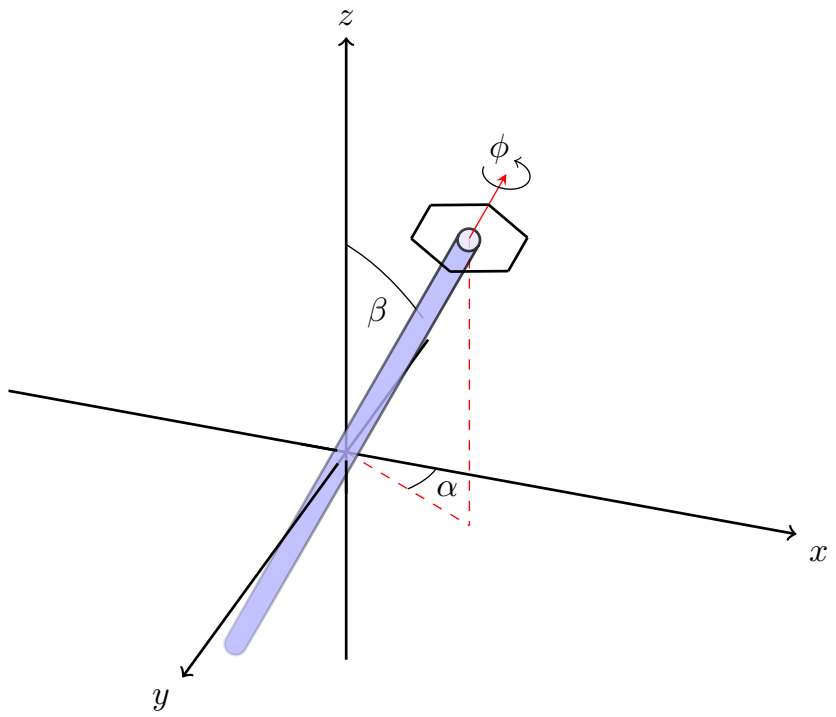

Figure S3. Schematic of a rod-like particle with arbitrary orientation with respect to a Cartesian co-ordinate system. The direction of the incoming X-rays is given by the positive x-axis

2. Supplementary Figures

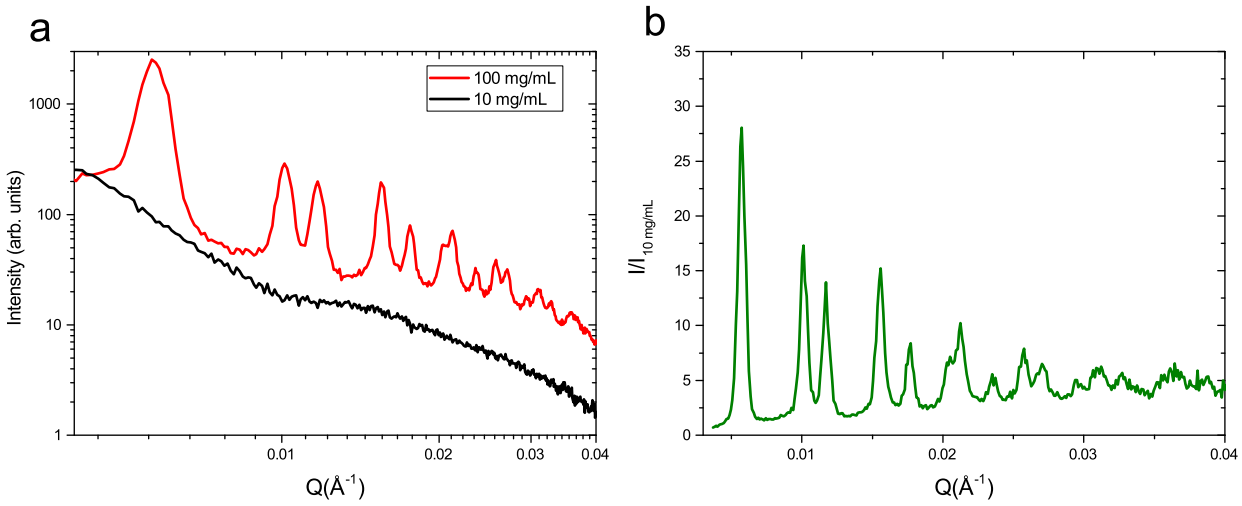

Figure S4. (a) Comparison of background subtracted and azimuthally averaged scattered intensity from small-angle X-ray scattering measurements of PFS_{133}-b-PI_{1250} micelles at high and low concentration. (b) The effective structure factor of PFS_{133}-b-PI_{1250} micelles at 100 mg/mL, found by taking the ratio of the 100 mg/mL and 10 mg/mL samples shown in (a).

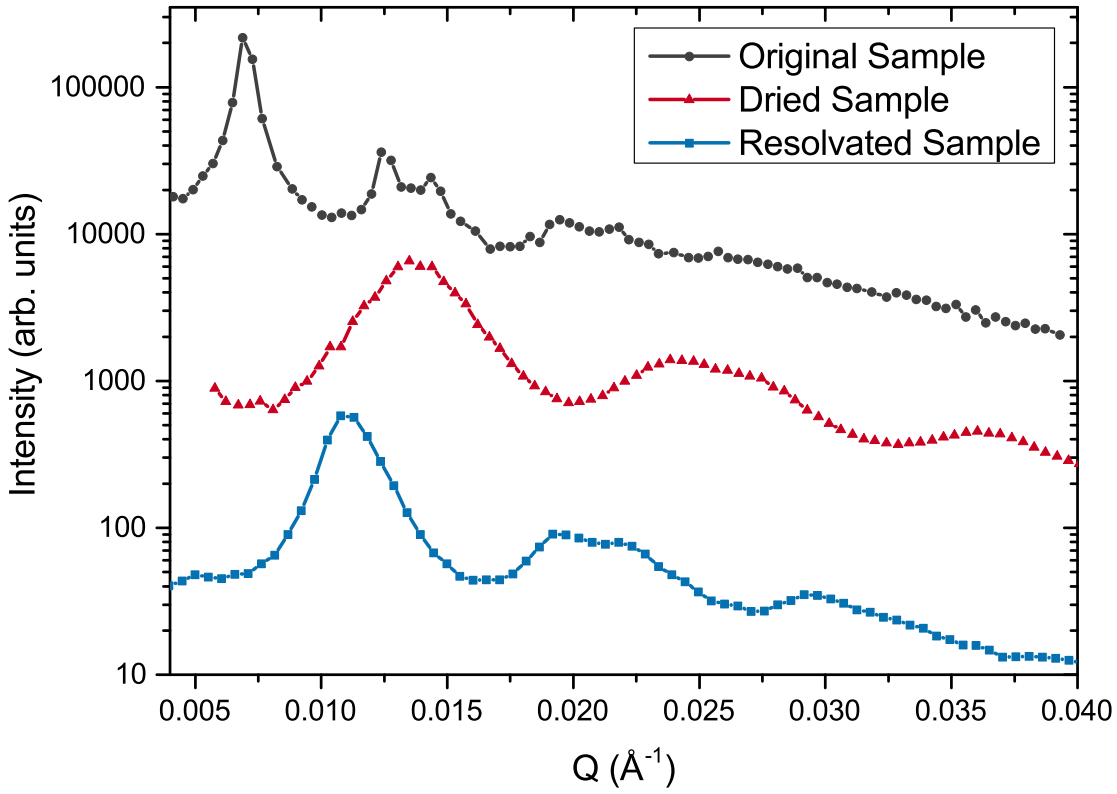

Figure S5. Comparison of scattering from original, dried sample and resolvated sample of PFS_{90}-*b*-PI_{890} micelles. The original concentration was 100 mg/mL, the sample was resolvated with approximately the same volume of decane but the exact concentration was not determined. The data are shifted arbitrarily in intensity for clarity.

References

[1] Hosemann R, Bagchi SN. Direct Analysis of Diffraction by Matter. Series in Physics; North-Holland Pub. Co.; 1962.

[2] Vaĭnshteĭn BK. Diffraction of X-rays by chain molecules. Chapter 5; Amsterdam and New York: Elsevier; 1966.

[3] Busson B, Doucet J. Distribution and interference functions for two-dimensional hexagonal paracrystals. Acta Crystallogr Sect A. 2000;56(1):68–72; doi: 10.1107/s0108767399011174.